Synthesis, characterization and crystal structure of 6-Chloro-4,4′-dimethyl-2,2′-bipyridine and 4,4′-Dimethyl 2,2′-bipyridine N-Oxide

Synthesis, characterization and crystal structure of 6-Chloro-4,4'-dimethyl-2,2'-bipyridine and 4,4'-Dimethyl 2,2'-bipyridine N-Oxide

Eleonora Conterosito,[a] Claudio Magistris,[b] Claudia Barolo,[b] Gianluca Croce[a*] and Marco Milanesio,[a*]

[a]Dipartimento di Scienze e Innovazione Tecnologica, Università del Piemonte Orientale, Viale T. Michel 11, Alessandria, 15121, Italy

[b]Dipartimento di Chimica, NIS Interdepartmental Centre, Università degli Studi di Torino, Via P. Giuria 7, Torino, 10125, Italy

Correspondence email: marco.milanesio@uniupo.it

Abstract

The synthesis, the NMR characterization and the crystal structure of 6-Chloro 4,4'-dimethyl 2,2'-bipyridine and of the reaction intermediate 4,4'-Dimethyl 2,2'-bipyridine N-Oxide are here reported. The target compound crystallizes in the orthorhombic system while the intermediate is monoclinic. In both structures, the molecules are linked by weak interactions. The structure of the reaction intermediate N-oxide is characterized by a dihedral angle between the two phenyl rings of 161.77° while the other is almost planar with a dihedral angle of 179.15°. The crystal packing was investigated, also with the aid of Hirshfeld surface analysis. In the N-oxide reaction intermediate the packing is governed by CH-O interactions, while in the product the packing is simply driven by minimizing the voids and thus maximizing the density, with a prevalence of H•••H and C•••H contacts, as indicated by fingerprint decomposition analysis.

1. Introduction

2,2'-Bipyridines have enjoyed considerable success as ligands in metal complexes, thanks to their ability to coordinate a variety of metal ions in different oxidation states.[1] Their simple structure favoured the application of a wide range of synthetic strategies, in order to extend the π-conjugated system and tune their physical and photochemical properties.[2–4] This resulted in a vast array of technological applications, ranging from solar energy conversion[5] to redox electrocatalysis.[6]

Unsymmetrically substituted 2,2'-bipyridines, in particular, retain a considerable interest in the possibility to tune the electronic properties in donor-acceptor conjugated systems, as well as in the construction of versatile metallo-supramolecular architectures.[7,8] In fact unsymmetrical substitution with a halogen

represents a preferred route to metal-catalysed cross-coupling reactions, typically used to extend the π-conjugation.

In this paper we report the synthesis and the structural determination of 6-chloro 4,4'-dimethyl 2,2'-bipyridine (**3**) and its synthetic intermediate 4,4'-dimethyl-2,2'-bipyridine N-oxide (**2**) together with their synthesis and characterization (MS, ^{1}H and ^{13}C NMR). 4,4'-Dimethyl-2,2'-bipyridine N-oxide (**2**), an intermediate in the synthesis of 4-(aminomethyl)-4'-methyl-2,2'-bipyridin dihydrochloride hydrate[3] and 4-(bromomethyl)-4'-methyl-2,2'-bipyridine dihydrobromide,[3] is usually synthesized by treatment of 4,4'-dimethyl 2,2'-bipyridine (**1**) with 3-chloroperbenzoic acid.[1,3] The synthesis of 6-Chloro 4,4'-dimethyl 2,2'-bipyridine (**3**) has been reported either by chlorination with $POCl_3$ of the N-oxide (**2**),[9] or through coupling of 2-chloropicoline with 2-bromopicoline.[10] It is a useful building block in the synthesis of 6-phosphanyl bipyridine ligands for electrochemical CO_2 reduction,[5] and tridentate azole-pyridine ligands for Co complexes.[11]

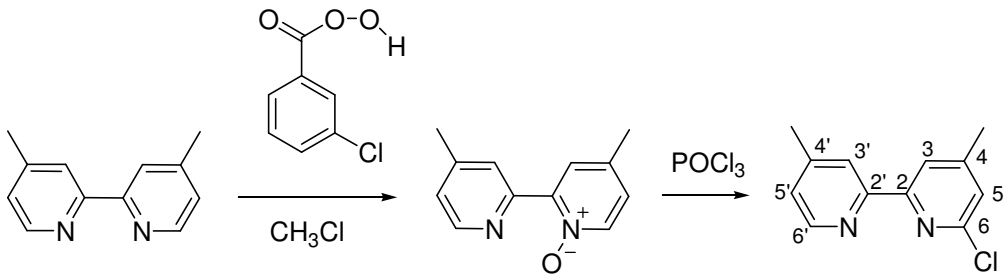

1 **2** **3**

Scheme 1 Synthesis route. 1st Step: oxidation of 4,4'-Dimethyl 2,2'-bipyridine (**1**) to 4,4'-Dimethyl 2,2'-bipyridine N-Oxide (**2**); 2nd Step: chlorination of the N-Oxide to 6-Chloro 4,4'-dimethyl 2,2'-bipyridine (**3**).

2. Experimental

2.1. Reactants and Instrumentation

All the chemicals were purchased from Sigma Aldrich and used without further purification. GC-MS spectra were recorded on a Thermo Finnigan Trace GC with a cross-linked methyl silicone capillary column, coupled to a Thermo Finnigan Trace MS mass spectrometer equipped with an electronic impact source (EI). ^{1}H NMR (200 MHz) and ^{13}C NMR (50 MHz) spectra were recorded on a Bruker Avance 200 NMR spectrometer.

2.2. Synthesis and crystallization

4,4'-Dimethyl 2,2'-bipyridine N-Oxide (2). A solution of freshly crystallized 3-chloroperbenzoic acid (31.30 g, 0.18 mol) in $CHCl_3$ (1.2 L) was slowly dropped (3 h) into a solution of 4,4'-Dimethyl 2,2'-bipyridine **1** (33.42 g, 0.18 mol) in $CHCl_3$ (0.6 L) in ice bath, and let under stirring at r.t. for 48 h. The solvent was evaporated and the residue neutralized with 1M K_2CO_3 and heated at 95 °C for 30 min, in order to filter the unreacted **1**; the solution was extracted with $CHCl_3$, dried over Na_2SO_4 and evaporated. The crude product (light brown solid, 27.97 g, η = 77%) was used in the following step; it was further purified by chromatography (EtOAc/MeOH = 9/1) before proceeding to crystallization. [1,6]

^{1}H-NMR ($CDCl_3$): δ = 8.70 (t, J = 0.8 Hz, $H_{3'}$), 8.54 (d, J = 5.0 Hz, $H_{6'}$), 8.18 (d, J = 6.7 Hz, H_6), 7.91 (d, J = 2.7, H_3), 7.14 (dq, $J_{5',6'}$ = 5.0, $J_{5',3'}$ = 0.8 Hz, $H_{5'}$), 7.04 (dd, $J_{5,6}$ = 6.7, $J_{5,3}$ = 2.7 Hz, H_5), 2.41 (s, CH_3), 2.36 (s, CH_3)[1,6]

^{13}C-NMR ($CDCl_3$): 149.7, 149.1, 147.6, 146.6, 140.1, 137.4, 128.4, 126.5, 126.59, 126.1, 125.3, 21.4, 20.5

GC-MS (EI): *m/z* (%) = 201 (41), 200 (77, M^+), 199 (77), 184 (70), 183 (68), 172 (62), 171 (100), 157 (40), 156 (58), 144 (69), 142 (32), 132 (81), 119 (65), 93 (37), 92 (72)

6-Chloro 4,4'-dimethyl 2,2'-bipyridine (3). Freshly distilled $POCl_3$ (50 mL) was carefully mixed with **2** (21.40 g, 0.11 mol) in ice bath, then let to room temperature under stirring and finally heated under reflux for 6 h. $POCl_3$ was distilled and, after cooling, the solid was cautiously poured in a becher containing ice (fumes); neutralized with Na_2CO_3 and extracted several times with CH_2Cl_2. The organic phase was dried over Na_2SO_4 and evaporated; elution with PE/EtOAc = 8/2 gave the pure product as white solid, g 18.70 (η = 80%)[9]

^{1}H-NMR ($CDCl_3$): δ= 8.47 (d, J = 5.0 Hz, H_{Ar}), 8.18 (s, H_{Ar}), 8.12 (s, H_{Ar}), 7.11-7.07 (m, $2H_{Ar}$), 2.38 (s, CH_3), 2.37 (s, CH_3)[9,10]

^{13}C-NMR ($CDCl_3$): 156.5, 154.5, 151.3, 150.9, 149.0, 148.3, 125.2, 124.6, 124.6, 122.3, 120.6, 120.6, 21.2, 21.0

GC-MS (EI): *m/z* (%) = 220 (43), 219 (39), 218 (100, M^+), 184 (38), 183 (93), 181 (37), 168 (35), 92 (44), 91 (33), 90 (34).

2.3. XRD data collection and refinement

Single-crystal diffraction data were collected using an Oxford Xcalibur CCD area detector diffractometer with graphite monochromator and Mo-Kα (λ =0.71069 Å) radiation. Data reduction and absorption corrections were performed using CrysAlisPRO[12] 171.34.44. Single crystal structure solution was performed by direct methods using SIR2011[13] and refinement with full-matrix least-squares employing SHELXL-2013[14] with ShelXle GUI[15]. Crystal data, data collection and structure refinement details are summarized in Table 1 and reported in details in Table S1-S4 and Table S5-S8 in the supplementary information file. H atoms were originally found in the difference Fourier map and then inserted in the model. All C-bound H atoms were then placed in the expected positions, with C-H = 0.97 (phenyl) or 0.95-1.00 Å (methyl), and refined as riding atoms on their carrier atoms, with $U_{iso}(H_{Ar}) = 1.2U_{eq}(C)$ for aromatic H atoms and $U_{iso}(H_{Me})$ $1.5U_{eq}(C)$ for methyl H atoms.[‡] Structural illustrations have been drawn with CCDC Mercury[16] and Crystal Explorer 3.1.[17] Crystal Explorer 3.1[17] was used to perform Hirshfeld surface analysis.

Table 1: Relevant crystallographic data of crystal structures of **2** and **3**.

Compound	**2**	**3**
Empirical formula	$C_{12}H_{12}N_2O$	$C_{12}H_{11}ClN_2$
Formula weight	200.24	218.68
Temperature	298 K	
Wavelength	0.71073 Å	
Crystal system	Monoclinic	Orthorhombic
Space group	P 21/n	P b c a
Unit cell dimensions	a = 7.3479(3) Å b = 11.8541(5) Å c = 12.0086(6) Å β= 97.160(4)°	a = 8.6128(8) Å b = 11.976(1) Å c = 21.591(3) Å
Volume	1037.83(8) $Å^3$	2227.1(4) $Å^3$
Z	4	8
Density (calculated)	1.282 Mg/m^3	1.304 Mg/m^3
Absorption coefficient	0.084 mm^{-1}	0.310 mm^{-1}
F(000)	424	912

[‡] Cif file of the structures of compound 2 and 3 were submitted to CCDC with numbers CCDC-1429846 and CCDC-1429847 respectively

Crystal size	0.4 x 0.3 x 0.2 mm^3	0.2 x 0.2 x 0.4 mm^3
Theta range for data collection	4.432 to 29.479°.	4.251 to 29.546°.
Independent reflections	2696 [R(int) = 0.0204]	2984 [R(int) = 0.0531]
Completeness to theta = 25.242°	99.4 %	99.6%
Data / restraints / parameters	2696 / 0 / 138	2984 / 0 / 150
Goodness-of-fit on F^2	1.041	1.011
Final R indices [I>2sigma(I)]	R1 = 0.0541, wR2 = 0.1369	R1 = 0.0688, wR2 = 0.1949
R indices (all data)	R1 = 0.0890, wR2 = 0.1589	R1 = 0.1367, wR2 = 0.2447

2.4. Hirshfeld analyses

Hirshfeld surfaces were generated by the program Crystal Explorer 3.1[17] All bond lengths to hydrogen were automatically modified to typical standard neutron values[18] (C-H = 1.083 Å, N-H = 1.009 Å and O-H = 0.983 Å), while the .CIF files of crystals 1-4 were read into the Crystal Explorer software program for calculations. We are aware that this analysis has some limitations for very weak interactions, like H•••H and C•••H contacts,[19] and the results were carefully checked by visual inspection of the crystal packing.

3. Results and discussion

6-Chloro 4,4'-dimethyl 2,2'-bipyridine (**3**) was synthesized as previously reported, through mono-oxidation of 4,4'-Dimethyl 2,2'-bipyridine (**1**) with 3-chloroperbenzoic acid,[1,6] and selective chlorination of the crude N-Oxide (**2**) with $POCl_3$.[9] All the products were characterized through MS and NMR spectroscopy.

The crystal structures of **2** and **3** were solved (structures and crystal packing features are reported Figure 1 and Figure 2 respectively) and compared with relevant literature data. The conformational features of the molecules and the packing of the molecule with (**2**) and without (**3**) the N-oxide moiety were analysed. The reaction product **3** crystallizes in Pbca (Figure 2) space group while **2** crystallizes in P21/n (Figure 1).

The first difference is observed at the molecular level is on the conformation of the phenyl groups. The dihedral angle between its two phenyl rings is close to 180° (179.15°) showing strong analogies with the structure of **1**.[20] Conversely, the intermediate compound **2** is not planar and the dihedral angle between the two rings is of 161.77°. This originates in **2** a short contact interaction of 2.315Å between the O1 atom on one molecule and the H15 and H9 atoms of two other molecules. It is possible to compare the structure of **2** with that of the symmetrical compound 4,4'-dimethyl-2,2'-bipyridine 1,1'-dioxide[21] (**4**) where the rotation

between the two rings is more accentuated forming a dihedral angle of 117.55°. By comparing the pyridine rings in the structures it is possible to see that, in both cases, they are planar but in the literature compound **4** the O atom of the N-oxide group is slightly out of the plane. Conversely, in our case it is almost in plane with a displacement of 0.04Å only.

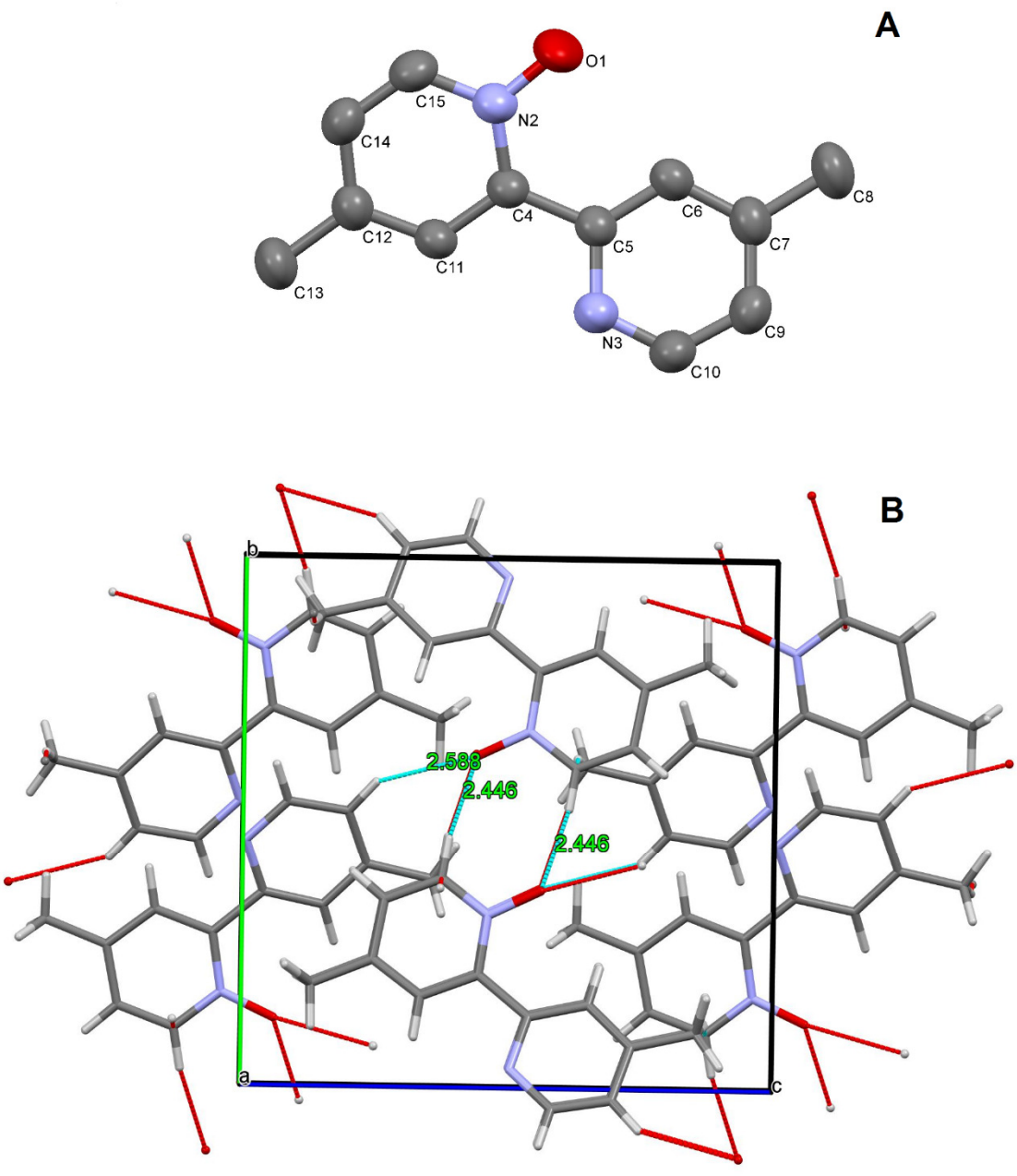

Figure 1 Crystal structure (A) and packing with relevant inter-molecular interactions (B) of compound **2**

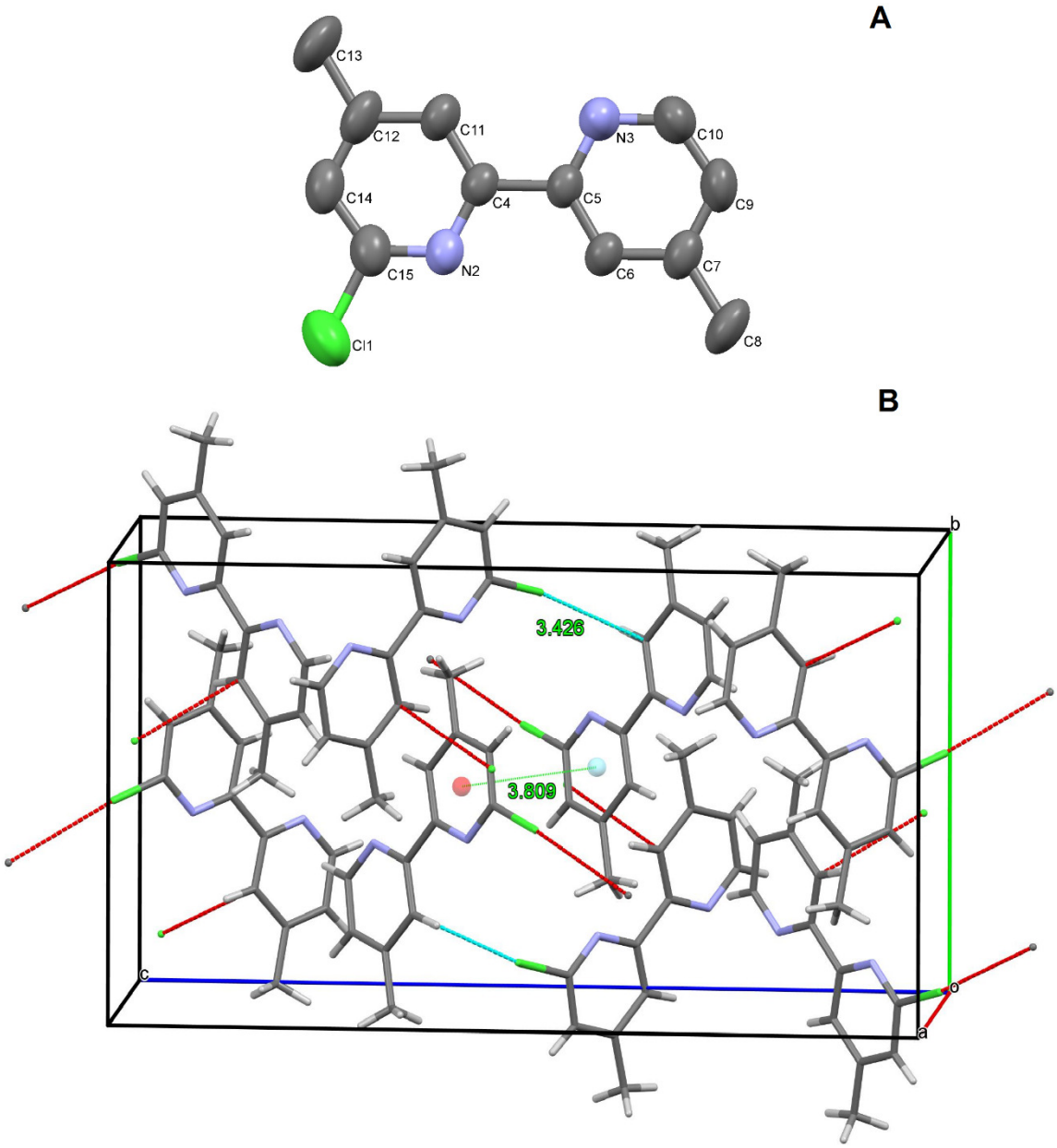

Figure 2 Crystal structure (A) and packing with relevant inter-molecular interactions (B) of compound **3**

The planarity and the presence of unconventional hydrogen bonds[22,23] can explain the different densities of compounds **1**, **2** ,**3** and **4**. Lower densities are associated to non-planar conformations and absence of CH•••O bonds. The presence of the N-oxide group in **2** breaks the symmetry of the molecule, stabilizing the non-planar conformation, and a less dense packing is observed (1.281 g/cm^3) with respect to **1** (1.322 g/cm^3), showing a planar conformation. The final product **3** shows intermediate density (1.304 g/cm^3), because it is

planar but no CH•••O bonds are observed. It is worth noting that in **4** higher densities (1.396 g/cm^3) are observed because several unconventional CH•••O hydrogen bonds are formed.

To further confirm the crystal packing driving forces, the Hirshfeld surfaces were generated and are shown in Figure 1 for the four compounds **1**, **2**, **3** and **4**. The Hirshfeld surfaces (Figure 3) highlight the intermolecular interactions better than the conventional packing pictures. The unique relevant contacts are the CH•••O bonded[24] contacts in compound **2** and **4**.

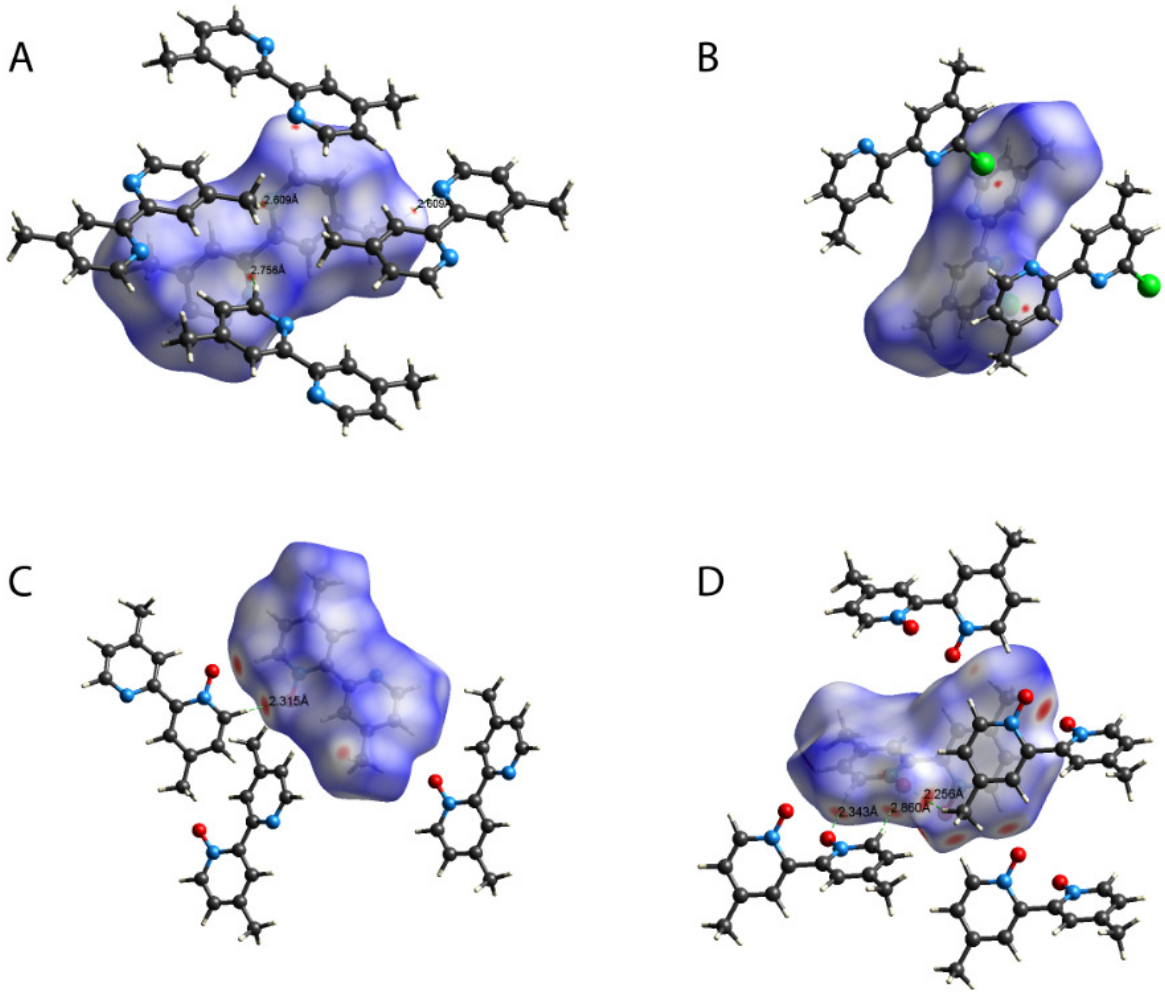

Figure 3 Hirshfeld surface (Isovalue 0.5) for **1** (A), **3** (B), **2** (C) and **4** (D). Neighbouring molecules associated with close contacts are shown along with distances between the atoms involved.

Fingerprint plots, reported in Figure 4 (while their decomposition is reported in ESI file, Figure S1), are in general rather flat without peculiar features (spots, densities in the low distances below 1.2 Å, asymmetrical features), and this confirms the dominance of weak interactions. In particular, for compound **1** it is flat,

symmetric and circular, with densities at the larger distances, and this indicates that the packing is driven by minimization of voids. In general, all four patterns do not show the presence of clear and relevant π-stacking interactions, that should be indicated by a red spot at the centre of the fingerprint plot, at about 1.8 Å, as can be seen in Figure 4, usually present in phenyl-rich molecules. Only for compound **3** and **4** a weak spot in the centre of Figure 4B and 4D suggests some degree of π-stacking, further confirmed by the inspection of peculiar flat zones in the curvedness of the Hirshfeld surfaces[25] (Figure 3B and 3D) and of the crystal packing. Conversely, Figure 2A and 2C do not show such flat portions in their surfaces. In compound **2** and **4,** the CH•••O bonds are confirmed by the spikes at the low distances in Figure 2C. Conversely, in compound **3** (Figure 4B) the absence of any significant feature indicates that the driving force of the packing is in both cases the minimization of the empty space. Compound **3** is similar to the reactant **1** and compound to **2** to compound **4**, the symmetrical dioxide. The decomposition of the fingerprint plots (see Figure 5 and Table S9 in ESI file for the numerical details) further confirms that the majority among the interactions are weak H•••H and C•••H contacts (beyond 75% in compound **1** and **2**, as expected from the chemical formula).

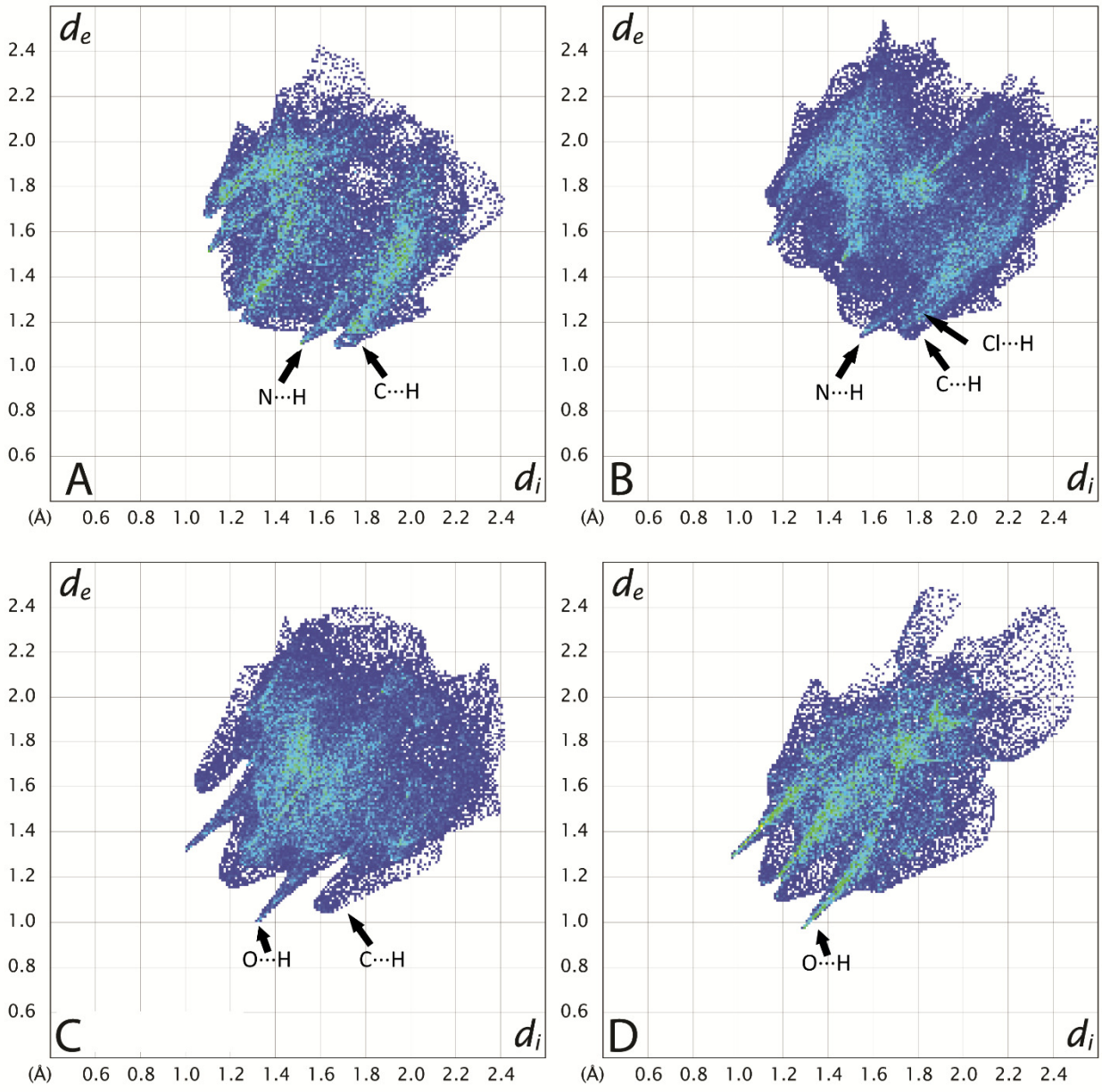

Figure 4 Fingerprint plots of **1** (A), **3** (B), **2** (C) and **4** (D).

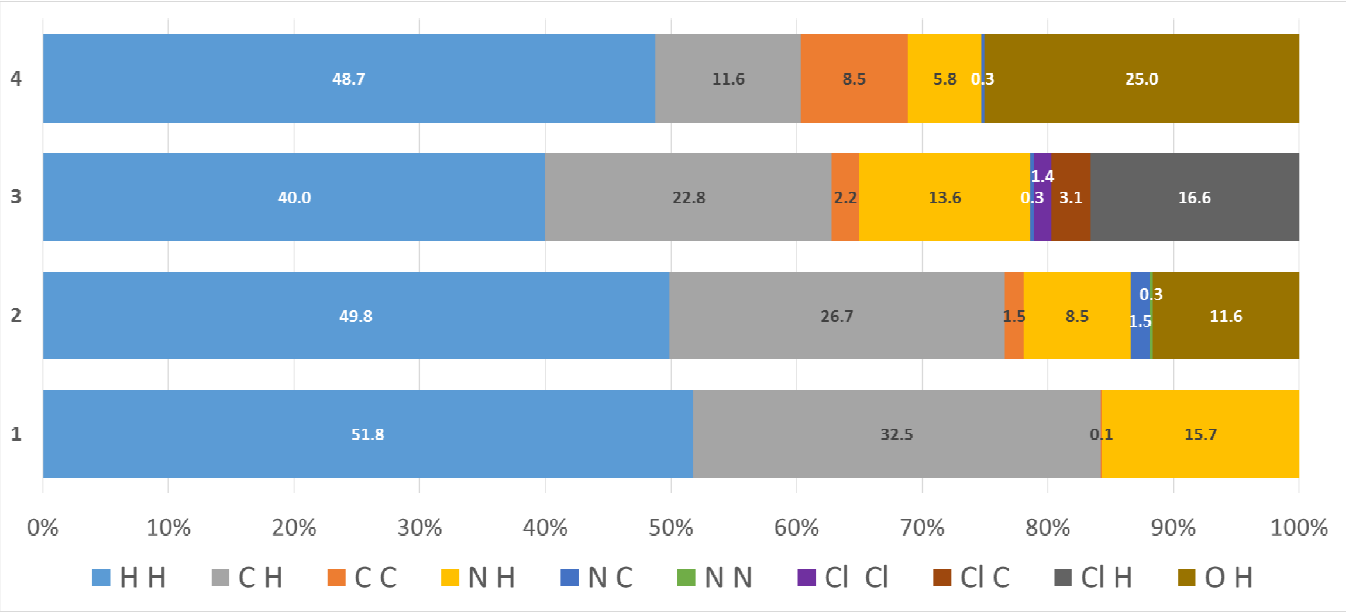

Figure 5 Distribution of intermolecular contacts from Hirshfeld surface analysis (%) for compound **1** – **4**.

4. Conclusions

The comparison among compound **3**, the reactant **1**, the intermediate N-oxide (**2**) and the symmetrical reference compound (**4**) allowed highlighting the features of the molecular interactions upon the change of the functional groups and symmetry. The formation of CH•••O unconventional hydrogen bonds is favoured, where possible, also by altering the molecule conformation (as in the oxidised compounds **2** and **4**, where the planarity of the molecule is broken), while in absence of these "not so weak" interactions the packing is driven by the maximization of the density and of the inter-molecular contacts. In all the studied cases, these CH•••O bonds and the minimization of empty spaces, with a predominance of H•••H and C•••H contacts as indicated by fingerprint decompositions and confirmed by the visual inspection of the crystal structures, are prevailing over π-stacking interactions. In compound **1**, the driving force of the crystal packing is the minimization of the empty space.

5. References

[1] Y. Xu, L. Duan, T. Åkermark, L. Tong, B.-L. Lee, R. Zhang, et al., Synthesis and catalytic water oxidation activities of ruthenium complexes containing neutral ligands, Chem. Eur. J. 17 (2011) 9520– 9528. doi:10.1002/chem.201100274.

[2] C. Barolo, M.K. Nazeeruddin, S. Fantacci, D. Di Censo, P. Comte, P. Liska, et al., Synthesis, characterization, and DFT-TDDFT computational study of a ruthenium complex containing a

functionalized tetradentate ligand., Inorg. Chem. 45 (2006) 4642–53. doi:10.1021/ic051970w.

[3] A. Abbotto, F. Sauvage, C. Barolo, F. De Angelis, S. Fantacci, M. Graetzel, et al., Panchromatic ruthenium sensitizer based on electron-rich heteroarylvinylene π-conjugated quaterpyridine for dye-sensitized solar cells., Dalton Trans. 40 (2011) 234–42. doi:10.1039/c0dt01190h.

[4] C. Barolo, J.-H. Yum, E. Artuso, N. Barbero, D. Di Censo, M.G. Lobello, et al., A simple synthetic route to obtain pure trans-ruthenium(II) complexes for dye-sensitized solar cell applications., ChemSusChem. 6 (2013) 2170–80. doi:10.1002/cssc.201200973.

[5] J. Park, G. Viscardi, C. Barolo, N. Barbero, Near-infrared sensitization in dye-sensitized solar cells., Chimia. 67 (2013) 129–35. doi:10.2533/chimia.2013.129.

[6] L. Della Ciana, I. Hamachi, T.J. Meyer, Synthesis of side-chain derivatives of 2,2'-bipyridine., J. Org. Chem. 54 (1989) 1731–1735. doi:10.1021/jo00268a042.

[7] M. Heller, U.S. Schubert, Functionalized 2,2‘-Bipyridines and 2,2‘:6‘,2‘ ‘-Terpyridines via Stille-Type Cross-Coupling Procedures., J. Org. Chem. 67 (2002) 8269–8272. doi:10.1021/jo0260600.

[8] A. Abbotto, C. Barolo, L. Bellotto, F. De Angelis, M. Grätzel, N. Manfredi, et al., Electron-rich heteroaromatic conjugated bipyridine based ruthenium sensitizer for efficient dye-sensitized solar cells., Chem. Commun. (Camb). (2008) 5318–20. doi:10.1039/b811378e.

[9] A.M. Lilio, K.A. Grice, C.P. Kubiak, A Series of Dinuclear Copper Complexes Bridged by Phosphanylbipyridine Ligands: Synthesis, Structural Characterization and Electrochemistry., Eur. J. Inorg. Chem. 2013 (2013) 4016–4023. doi:10.1002/ejic.201201208.

[10] Y. Wang, (Jsr Corporation, Japan) Patent, WO2008059960

[11] N.M. Shavaleev, F. Kessler, M. Grätzel, M.K.M.K. Nazeeruddin, Redox properties of cobalt(II) complexes with azole-pyridines., Inorganica Chim. Acta. 407 (2013) 261–268. doi:10.1016/j.ica.2013.07.057.

[12] Crysalis CCD and Crysalis RED Versions 1.171.34.44, Agilent Technologies Oxford U.K. (2006).

[13] M.C. Burla, R. Caliandro, M. Camalli, B. Carrozzini, G.L. Cascarano, C. Giacovazzo, et al., SIR2011□: a new package for crystal structure determination and refinement., J. Appl. Crystallogr. 45 (2012) 357–361. doi:10.1107/S0021889812001124.

[14] G.M. Sheldrick, SHELXL-2013 Acta Crystallogr. Sect. A. 64 (2008) 112–122.

[15] C.B. Hübschle, G.M. Sheldrick, B. Dittrich, ShelXle: a Qt graphical user interface for SHELXL., J. Appl. Crystallogr. 44 (2011) 1281–1284. doi:10.1107/S0021889811043202.

[16] C.F. Macrae, P.R. Edgington, P. McCabe, E. Pidcock, G.P. Shields, R. Taylor, et al., Mercury: visualization and analysis of crystal structures., J. Appl. Cryst. 39 (2006) 453–457.

[17] S.K. Wolff, D.J. Grimwood, J.J. McKinnon, D. Jayatilaka, M.A. Spackman, Crystal Explorer, (2007). http://hirshfeldsurface.net/CrystalExplorer.

[18] F.H. Allen, O. Kennard, D.G. Watson, L. Brammer, A.G. Orpen, R. Taylor, Tables of bond lengths determined by X-ray and neutron diffraction. Part 1. Bond lengths in organic compounds., J. Chem. Soc. Perkin Trans. 2. (1987) S1. doi:10.1039/p298700000s1.

[19] A.D. Martin, J. Britton, T.L. Easun, A.J. Blake, W. Lewis, M. Schröder, Hirshfeld Surface Investigation of Structure-Directing Interactions within Dipicolinic Acid Derivatives., Cryst. Growth Des. (2015) 150320074652002. doi:10.1021/cg5016934.

[20] P. Pearson, C.M. Kepert, G.B. Deacon, L. Spiccia, A.C. Warden, B.W. Skelton, et al., Synthesis of heteroleptic bis(diimine)carbonylchlororuthenium(II) complexes from photodecarbonylated precursors., Inorg. Chem. 43 (2004) 683.

[21] H. Kanno, K. Iijima, Acta Crystallogr. Sect.C Cryst.Struct.Commun. 53 (1997) 498.

[22] S. Aime, E. Diana, R. Gobetto, M. Milanesio, E. Valls, D. Viterbo, Structural and Spectroscopic Study of the Dihydrogen Bond in an Imine Triosmium Complex, Organometallics. 21 (2002) 50–57.

[23] S. Aime, F. Bertone, R. Gobetto, L. Milone, A. Russo, M.J. Stchendroff, et al., The Effect of Ligand Basicity on the Unconventional Hydrogen-Bond in H(μ-H)Os3(CO)10L (L = amine) Derivatives, Inorganica Chim. Acta. 334 (2002) 448–454.

[24] C. Gatti, Chemical bonding in crystals□: new directions, Z. Krist. 220 (2005) 399–457.

[25] M.A. Spackman, D. Jayatilaka, Hirshfeld surface analysis, Cryst. Eng. Comm. 11 (2009) 19–32. doi:10.1039/b818330a.